Electromagnetic Scattering from Multiple Rectangular Apertures in a Thick Conducting Screen

Hyun Ho Park and Hyo Joon Eom, *Member, IEEE*

***Abstract*—Electromagnetic wave scattering from multiple rectangular apertures in a thick conducting screen is studied. The Fourier-transform and mode-matching technique are used to obtain simultaneous equations for the modal coefficients. The simultaneous equations are solved to represent the scattered and transmitted fields in series forms which are suitable for numerical computation. The numerical computations are performed to illustrate the aperture transmission and scattering behaviors in terms of aperture size, incident angle, and frequency. The effects of the finite number of apertures on the transmission characteristics are discussed.**

***Index Terms*—Apertures, electromagnetic scattering.**

I. Introduction

ELECTROMAGNETIC penetration into an aperture in a conducting plane has been of importance in EMI/EMC-related problems. Electromagnetic scattering from a rectangular aperture in a thin conducting plane has been recently studied with an operator equation [1]. Electromagnetic scattering from a rectangular cavity and aperture in a thick conducting plane are also extensively studied in [2] and [3] using the finite-element method. A conducting plate perforated with multiple apertures has been widely used as a microwave frequency selective surface. The method of moments and the Floquet space harmonics have been applied to solve the integral equation for scattering from infinite number of apertures in thick conducting screen [4]. The method of moments has been also used for computing the magnetic current on the finite number of apertures in an infinitely thin conducting plate [5], [6].

In this paper, we provide a formulation for electromagnetic scattering from multiple rectangular apertures in a thick conducting screen, by using the Fourier transform and mode matching as used in [7]. The Fourier transform and mode-matching method were also used to study electrostatic penetration into a rectangular aperture and a slit in a conducting plane [8], [9]. The solution presented in the paper is a fast-converging series form that is numerically efficient and reduces to a closed form in high-frequency limit for a single aperture. The organization of the paper is as follows. In the next two sections, we show the expressions for the scattered and transmitted fields in the spectral domain by using the boundary conditions. In Section IV, we perform the numerical calculations and compare them with other existing solutions. A brief summary is given in Section V.

Manuscript received October 13, 1997.

The authors are with the Department of Electrical Engineering, Korea Advanced Institute of Science and Technology, Yusung Gu, Taejon, 305-701 Korea.

Publisher Item Identifier S 0018-926X(99)05815-9.

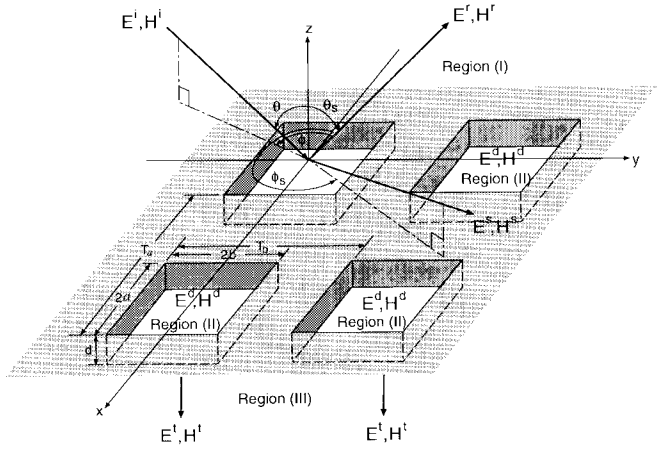

Fig. 1. Geometry of scattering problem.

II. Field Representation

Consider $(M_l+1)\times(M_k+1)$ number of multiple rectangular apertures with area $2a \times 2b$, thickness d in Fig. 1. Assume that T_a and T_b are the periods in the x and y directions, respectively. An electromagnetic wave is obliquely incident on the rectangular aperture. In region (I), the incident and reflected E-fields are

$$\vec{E}^i = Z_0\{(u\sin\phi + v\cos\phi\cos\theta)\hat{x} - (u\cos\phi - v\sin\phi\cos\theta)\hat{y} + v\sin\theta\hat{z}\}e^{ik_x x + ik_y y - ik_z z} \quad (1)$$

$$\vec{E}^r = -Z_0\{(u\sin\phi + v\cos\phi\cos\theta)\hat{x} - (u\cos\phi - v\sin\phi\cos\theta)\hat{y} - v\sin\theta\hat{z}\}e^{ik_x x + ik_y y + ik_z z} \quad (2)$$

where $\hat{x}$, $\hat{y}$, and $\hat{z}$ are the unit vectors, $k_x = k_0\cos\phi\sin\theta$, $k_y = k_0\sin\phi\sin\theta$, $k_z = k_0\cos\theta$, $k_0 = \omega\sqrt{\mu_0\epsilon_0} = 2\pi/\lambda$ is the wave number, and $Z_0 = \sqrt{\mu_0/\epsilon_0}$ is the free-space intrinsic impedance. The polarization state of the incident field is determined by u and v.

The scattered $\vec{E}^{s,t}$- and $\vec{H}^{s,t}$-fields in regions (I) and (III) are represented by the z components of the electric and magnetic vector potentials $F_z^{s,t}(x, y, z)$ and $A_z^{s,t}(x, y, z)$, respectively [10]. Note that the superscripts s and t are used

to designate the vector potentials in regions (I) and (III)

$$F_z^s(x, y, z) = \frac{1}{4\pi^2}\int_{-\infty}^{\infty}\int_{-\infty}^{\infty}\tilde{F}_z^s(\zeta, \eta)e^{-i\zeta x - i\eta y + i\kappa z}\,d\zeta\,d\eta \quad (3)$$

$$F_z^t(x, y, z) = \frac{1}{4\pi^2}\int_{-\infty}^{\infty}\int_{-\infty}^{\infty}\tilde{F}_z^t(\zeta, \eta)e^{-i\zeta x - i\eta y - i\kappa(z+d)}\,d\zeta\,d\eta \quad (4)$$

where $\kappa^2 = k_0^2 - \zeta^2 - \eta^2$. Assume $\tilde{F}_z^s(\zeta, \eta)$ and $\tilde{F}_z^t(\zeta, \eta)$ are the Fourier transforms of $F_z^s(x, y, 0)$ and $F_z^t(x, y, -d)$ given by $\tilde{F}_z^s(\zeta, \eta) = \int_{-\infty}^{\infty}\int_{-\infty}^{\infty}F_z^s(x, y, 0)e^{i\zeta x + i\eta y}\,dx\,dy$, $\tilde{F}_z^t(\zeta, \eta) = \int_{-\infty}^{\infty}\int_{-\infty}^{\infty}F_z^t(x, y, -d)e^{i\zeta x + i\eta y}\,dx\,dy$. $A_z^s(x, y, z)$ and $A_z^t(x, y, z)$ are similarly defined.

In region (II), (lth and kth aperture in the x and y directions) the vector potentials $F_z^d(x, y, z)$ and $A_z^d(x, y, z)$ within the rectangular aperture are

$$F_z^d(x, y, z) = \sum_{m=0}^{\infty}\sum_{n=0}^{\infty}[c_{mn}^{lk}\cos\xi_{mn}(z+d) + d_{mn}^{lk}\sin\xi_{mn}(z+d)]\cos a_m(x - lT_a + a)\cdot\cos b_n(y - kT_b + b) \quad (5)$$

$$A_z^d(x, y, z) = \sum_{m=1}^{\infty}\sum_{n=1}^{\infty}[\bar{c}_{mn}^{lk}\cos\xi_{mn}(z+d) + \bar{d}_{mn}^{lk}\sin\xi_{mn}(z+d)]\sin a_m(x - lT_a + a)\cdot\sin b_n(y - kT_b + b) \quad (6)$$

where $(m, n) \neq (0, 0)$, $\xi_{mn} = \sqrt{k_1^2 - a_m^2 - b_n^2}$, $k_1 = \omega\sqrt{\mu_1\epsilon_1}$, $a_m = m\pi/(2a)$, and $b_n = n\pi/(2b)$.

III. Boundary Conditions

To determine the unknown coefficients c_{mn}^{lk}, d_{mn}^{lk}, $\bar{c}_{mn}^{lk}$, and $\bar{d}_{mn}^{lk}$ we enforce the boundary conditions on the $E_{x,y}$ and $H_{x,y}$ continuities at $z = 0$ and $-d$.

First, we apply the boundary conditions on $E_{x,y}$ and $H_{x,y}$ at $z = 0$.

$$E_{x,y}^i(x, y, 0) + E_{x,y}^r(x, y, 0) + E_{x,y}^s(x, y, 0) = \begin{cases} E_{x,y}^d(x, y, 0), & \text{for } |x - lT_a| < a,\ |y - kT_b| < b \\ 0, & \text{otherwise} \end{cases} \quad (7)$$

and

$$H_{x,y}^i(x, y, 0) + H_{x,y}^r(x, y, 0) + H_{x,y}^s(x, y, 0) = H_{x,y}^d(x, y, 0) \quad \text{for } |x - lT_a| < a,\ |y - kT_b| < b. \quad (8)$$

Applying the Fourier transform to (7) and solving for $\tilde{F}_z^s(\zeta, \eta)$ and $\tilde{A}_z^s(\zeta, \eta)$, we obtain

$$\tilde{F}_z^s(\zeta, \eta) = -\frac{(ab)^2\epsilon_0}{\epsilon_1}\sum_{l=0}^{M_l}\sum_{k=0}^{M_k}\sum_{m=0}^{\infty}\sum_{n=0}^{\infty}\frac{\zeta\eta(a_m^2 + b_n^2)}{\zeta^2 + \eta^2}\cdot[c_{mn}^{lk}\cos(\xi_{mn}d) + d_{mn}^{lk}\sin(\xi_{mn}d)]\cdot K_m(\zeta a)K_n(\eta b)e^{i\zeta lT_a + i\eta kT_b} \quad (9)$$

$$\tilde{A}_z^s(\zeta, \eta) = \frac{(ab)^2\omega\mu_0\epsilon_0}{\epsilon_1}\sum_{l=0}^{M_l}\sum_{k=0}^{M_k}\sum_{m=0}^{\infty}\sum_{n=0}^{\infty}\frac{(a_m^2\eta^2 - b_n^2\zeta^2)}{(\zeta^2 + \eta^2)\kappa}\cdot[c_{mn}^{lk}\cos(\xi_{mn}d) + d_{mn}^{lk}\sin(\xi_{mn}d)]\cdot K_m(\zeta a)K_n(\eta b)e^{i\zeta lT_a + i\eta kT_b} + \frac{i(ab)^2\mu_0\epsilon_0}{\mu_1\epsilon_1}\sum_{l=0}^{M_l}\sum_{k=0}^{M_k}\sum_{m=1}^{\infty}\sum_{n=1}^{\infty}\frac{a_m b_n\xi_{mn}}{\kappa}\cdot[\bar{c}_{mn}^{lk}\sin(\xi_{mn}d) - \bar{d}_{mn}^{lk}\cos(\xi_{mn}d)]K_m(\zeta a)\cdot K_n(\eta b)e^{i\zeta lT_a + i\eta kT_b} \quad (10)$$

where

$$K_m(u) = \frac{(-1)^m e^{iu} - e^{-iu}}{u^2 - \left(\frac{m\pi}{2}\right)^2}. \quad (11)$$

Substituting (9) and (10) into (8), multiplying (8) by $\cos a_p(x - rT_a + a)\sin b_q(y - wT_b + b)$ or $\sin a_p(x - rT_a + a)\cos b_q(y - wT_b + b)$, and performing integration over the area of the aperture, we obtain the simultaneous equations for c_{mn}^{lk}, d_{mn}^{lk}, $\bar{c}_{mn}^{lk}$, and $\bar{d}_{mn}^{lk}$

$$\begin{aligned}\gamma_{pq}^{rw} &+ \frac{(ab)^3 b_q}{4\pi^2}\sum_{l=0}^{M_l}\sum_{k=0}^{M_k}\sum_{m=0}^{\infty}\sum_{n=0}^{\infty}[c_{mn}^{lk}\cos(\xi_{mn}d) + d_{mn}^{lk}\sin(\xi_{mn}d)]\left\{\frac{\omega\epsilon_0}{\epsilon_1}b_n^2 I_2 - \frac{(a_m^2 + b_n^2)}{\omega\mu_0\epsilon_1}I_1\right\} \\ &- \frac{i(ab)^3\epsilon_0 b_q}{4\pi^2\mu_1\epsilon_1}\sum_{l=0}^{M_l}\sum_{k=0}^{M_k}\sum_{m=1}^{\infty}\sum_{n=1}^{\infty}[\bar{c}_{mn}^{lk}\sin(\xi_{mn}d) - \bar{d}_{mn}^{lk}\cos(\xi_{mn}d)]a_m b_n\xi_{mn}I_2 \\ &= \frac{i\varepsilon_p b_q}{\omega\mu_1\epsilon_1}[c_{pq}^{rw}\sin(\xi_{pq}d) - d_{pq}^{rw}\cos(\xi_{pq}d)]\cdot\xi_{pq}\,\delta_{mp}\,\delta_{nq}\,\delta_{lr}\,\delta_{kw} - \frac{\varepsilon_p a_p}{\mu_1}[\bar{c}_{pq}^{rw}\cos(\xi_{pq}d) + \bar{d}_{pq}^{rw}\sin(\xi_{pq}d)]\delta_{mp}\,\delta_{nq}\,\delta_{lr}\,\delta_{kw} \end{aligned} \quad (12)$$

$$\begin{aligned}\bar{\gamma}_{pq}^{rw} &+ \frac{(ab)^3 a_p}{4\pi^2}\sum_{l=0}^{M_l}\sum_{k=0}^{M_k}\sum_{m=0}^{\infty}\sum_{n=0}^{\infty}[c_{mn}^{lk}\cos(\xi_{mn}d) + d_{mn}^{lk}\sin(\xi_{mn}d)]\cdot\left\{\frac{\omega\epsilon_0}{\epsilon_1}a_m^2 I_3 - \frac{(a_m^2 + b_n^2)}{\omega\mu_0\epsilon_1}I_1\right\} \\ &+ \frac{i(ab)^3\epsilon_0 a_p}{4\pi^2\mu_1\epsilon_1}\sum_{l=0}^{M_l}\sum_{k=0}^{M_k}\sum_{m=1}^{\infty}\sum_{n=1}^{\infty}[\bar{c}_{mn}^{lk}\sin(\xi_{mn}d) - \bar{d}_{mn}^{lk}\cos(\xi_{mn}d)]a_m b_n\xi_{mn}I_3 \\ &= \frac{i\varepsilon_q a_p}{\omega\mu_1\epsilon_1}[c_{pq}^{rw}\sin(\xi_{pq}d) - d_{pq}^{rw}\cos(\xi_{pq}d)]\cdot\xi_{pq}\,\delta_{mp}\,\delta_{nq}\,\delta_{lr}\,\delta_{kw} + \frac{\varepsilon_q b_q}{\mu_1}[\bar{c}_{pq}^{rw}\cos(\xi_{pq}d) + \bar{d}_{pq}^{rw}\sin(\xi_{pq}d)]\delta_{mp}\,\delta_{nq}\,\delta_{lr}\,\delta_{kw} \end{aligned} \quad (13)$$

where $\varepsilon_0 = 2$, $\varepsilon_1 = \varepsilon_2 = \cdots = 1$, and

$$\gamma_{pq}^{rw} = 2iab(u\sin\phi\cos\theta + v\cos\phi)k_x b_q K_p(k_x a)K_q(k_y b)\cdot e^{ik_x rT_a + ik_y wT_b} \quad (14)$$

$$\bar{\gamma}_{pq}^{rw} = 2iab(u\cos\phi\cos\theta - v\sin\phi)k_y a_p K_p(k_x a)K_q(k_y b)\cdot e^{ik_x rT_a + ik_y wT_b} \quad (15)$$

$$I_{1,2,3} = \int_{-\infty}^{\infty}\int_{-\infty}^{\infty} \Omega_{1,2,3}\,\frac{L(\zeta,\eta)}{\kappa} \cdot e^{i\zeta(l-r)T_a + i\eta(k-w)T_b}\,d\zeta\,d\eta \tag{16}$$

where $\Omega_1 = \zeta^2\eta^2$, $\Omega_2 = \zeta^2$, $\Omega_3 = \eta^2$, and $L(\zeta,\eta) = K_m(\zeta a)K_p(-\zeta a)K_n(\eta b)K_q(-\eta b)$. The efficient numerical evaluations of $I_{1,2,3}$ are possible by using the quadrature method used in [11].

In high-frequency limit for a single aperture ($M_l = M_k = 0$), $I_{1,2,3}$ have main contributions from the poles of $L(\zeta,\eta)$ at $m = p$ and $n = q$

$$I_{1,2,3} \to \frac{4\pi^2}{(ab)^3}\,\frac{\overline{\Omega}_{1,2,3}}{\xi_{pq}}\,\delta_{mp}\,\delta_{nq} \tag{17}$$

where $\overline{\Omega}_1 = \varepsilon_p\varepsilon_q$, $\overline{\Omega}_2 = \varepsilon_p/b_q^2$, and $\overline{\Omega}_3 = \varepsilon_q/a_p^2$. This means that the high-frequency approximate solution for a single aperture is represented in analytic closed form, thereby significantly reducing a computational amount.

Similarly, from the boundary conditions on $E_{x,y}$ and $H_{x,y}$ at $z = -d$, we obtain the simultaneous equations for c_{mn}^{lk}, d_{mn}^{lk}, $\overline{c}_{mn}^{lk}$, and $\overline{d}_{mn}^{lk}$

$$\frac{(ab)^3 b_q}{4\pi^2}\sum_{l=0}^{M_l}\sum_{k=0}^{M_k}\sum_{m=0}^{\infty}\sum_{n=0}^{\infty} c_{mn}^{lk}\left\{\frac{\omega\epsilon_0}{\epsilon_1}\,b_n^2 I_2 - \frac{(a_m^2+b_n^2)}{\omega\mu_0\epsilon_1}\,I_1\right\} + \frac{i(ab)^3\epsilon_0 b_q}{4\pi^2\mu_1\epsilon_1}\sum_{l=0}^{M_l}\sum_{k=0}^{M_k}\sum_{m=1}^{\infty}\sum_{n=1}^{\infty}\overline{d}_{mn}^{lk}a_m b_n\xi_{mn}I_2 = \frac{i\varepsilon_p b_q}{\omega\mu_1\epsilon_1}\,d_{pq}^{rw}\xi_{pq}\,\delta_{mp}\,\delta_{nq}\,\delta_{lr}\,\delta_{kw} + \frac{\varepsilon_p a_p}{\mu_1}\,\overline{c}_{pq}^{rw} \cdot \delta_{mp}\,\delta_{nq}\,\delta_{lr}\,\delta_{kw} \tag{18}$$

$$\frac{(ab)^3 a_p}{4\pi^2}\sum_{l=0}^{M_l}\sum_{k=0}^{M_k}\sum_{m=0}^{\infty}\sum_{n=0}^{\infty} c_{mn}^{lk}\left\{\frac{\omega\epsilon_0}{\epsilon_1}\,a_m^2 I_3 - \frac{(a_m^2+b_n^2)}{\omega\mu_0\epsilon_1}\,I_1\right\} - \frac{i(ab)^3\epsilon_0 a_p}{4\pi^2\mu_1\epsilon_1}\sum_{l=0}^{M_l}\sum_{k=0}^{M_k}\sum_{m=1}^{\infty}\sum_{n=1}^{\infty}\overline{d}_{mn}^{lk}a_m b_n\xi_{mn}I_3 = \frac{i\varepsilon_q a_p}{\omega\mu_1\epsilon_1}\,d_{pq}^{rw}\xi_{pq}\,\delta_{mp}\,\delta_{nq}\,\delta_{lr}\,\delta_{kw} - \frac{\varepsilon_q b_q}{\mu_1}\,\overline{c}_{pq}^{rw}\,\delta_{mp} \cdot \delta_{nq}\,\delta_{lr}\,\delta_{kw}. \tag{19}$$

In case of a single aperture ($M_l = M_k = 0$), the field expressions (12), (13), (18), and (19) reduce to simple forms with $l = k = r = w = 0$. This means that the summations over l and k vanish.

If the region (III) is filled with the perfect conductor (i.e., rectangular cavities), the field representations associated with $F_z^t(x, y, z)$ and $A_z^t(x, y, z)$ are unnecessary. By matching the boundary conditions with (3), (5), and (6) at $z = 0$ we obtain (12) and (13) with $c_{mn}^{lk} = \overline{d}_{mn}^{lk} = 0$.

If $d \to \infty$, we obtain (12) and (13) with $d_{mn}^{lk} = -ic_{mn}^{lk}$ and $\overline{d}_{mn}^{lk} = -i\overline{c}_{mn}^{lk}$.

IV. Numerical Computations

The angular behaviors of radar cross section (RCS) from a rectangular aperture are extensively studied in [3]. In order to check the accuracy of our formulation, we evaluated the backscattered RCS of a single aperture for $u = 0$, $v = 1$, and $u = 1$, $v = 0$ cases where $2a/\lambda = 0.4$, $2b/\lambda = 0.4$, and $d/\lambda = 0.25$. We compared our result with [3, fig. 5] and confirmed excellent agreement.

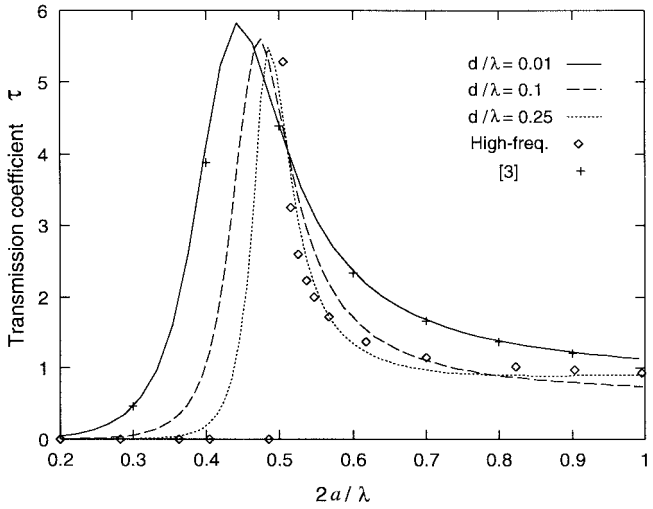

Fig. 2. Transmission coefficient versus aperture length $2a/\lambda$: $2b/\lambda = 0.1$, $u = 1$, $v = 0$, $\phi = \theta = 0^\circ$, $k_1 = k_0$.

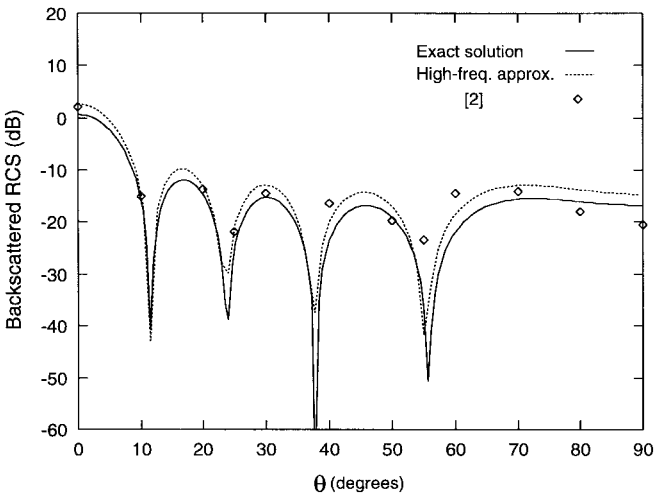

Fig. 3. Angular behavior of backscattered RCS for rectangular cavity $2a/\lambda = 2.5$, $2b/\lambda = 0.25$, $d/\lambda = 0.25$, $u = 0$, $v = 1$, $\phi = 0^\circ$, $k_1 = k_0$.

The transmission coefficient τ of the aperture is defined as a ratio of the total power transmitted through the aperture to the power incident on the aperture.

In Fig. 2, we show the transmission coefficient τ versus size $2a/\lambda$ for a rectangular aperture of size $2b/\lambda = 0.1$. Our results for $d/\lambda = 0.01, 0.1$, and 0.25 agree well with [3]. In our computation, we used $m = n = 3$ when $2a/\lambda = 0.5$ in (12), (13), (18), and (19). Our computational experience indicates that the number of modes m and n used in the simultaneous equations (12), (13), (18), and (19) must be at least the number of the propagation modes given by $(2/\lambda)^2 > (m/2a)^2 + (n/2b)^2$ plus a few higher evanescent modes. It is interesting to note that our high-frequency solution based on (17), which is independent of aperture depth d, gives reasonable results for $d/\lambda \geq 0.25$ when $2a/\lambda > 0.5$.

In Fig. 3, we show the angular behavior of the backscattered RCS for a rectangular cavity. Our result agrees well with [2]. Note that our high-frequency solution based on (17) also gives a rather accurate result owing to a rather large size $2a/\lambda = 2.5$.

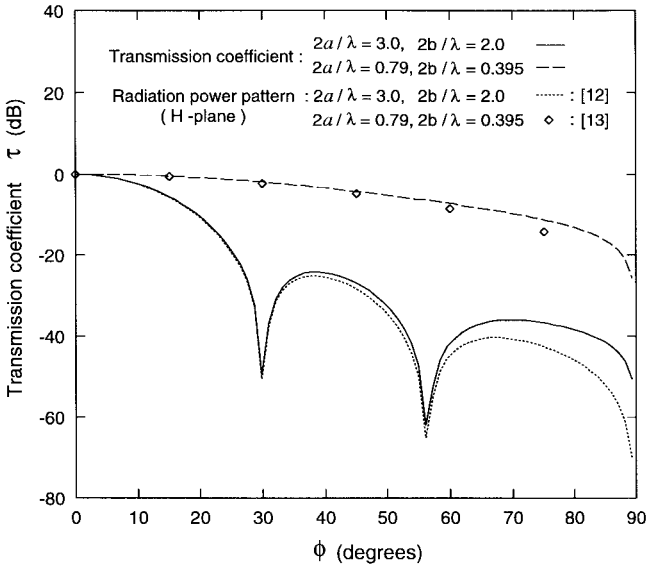

Fig. 4. Angular behavior of transmission coefficient for flanged rectangular waveguide: $u = 1$, $v = 0$, $\phi = 0°$, $k_1 = k_0$.

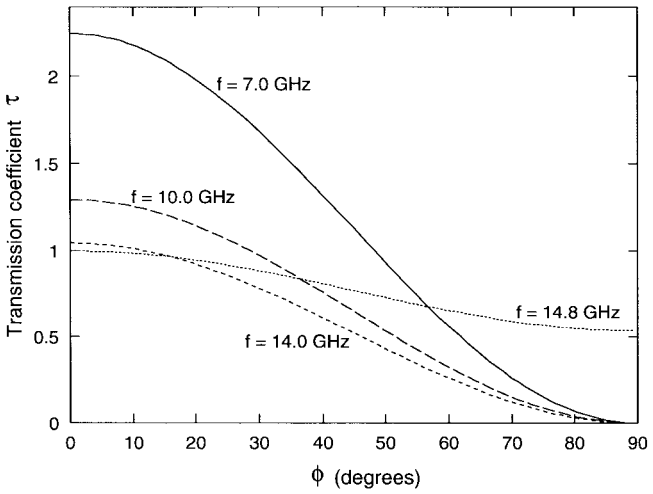

Fig. 5. Angular behavior of transmission coefficient for flanged rectangular waveguide: $a = 1.143$ cm, $b = 0.508$ cm, $u = 1$, $v = 0$, $\theta = 0°$, $k_1 = k_0$.

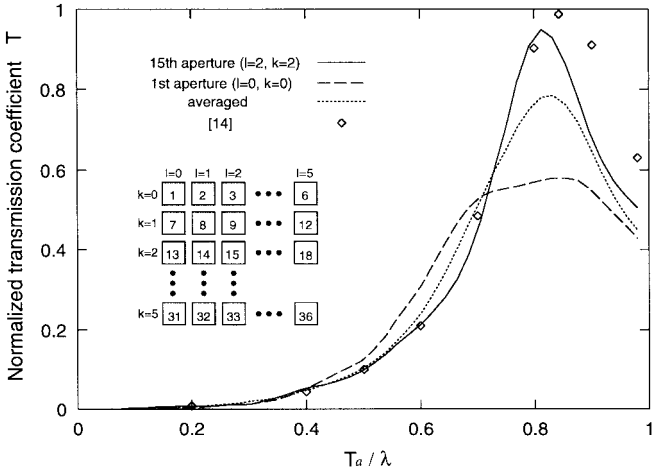

Fig. 6. Normalized transmission coefficient versus the normalized frequency at normal incidence: $2a = 0.7 \times T_a$, $d = 0.2 \times T_a$, $b = a$, $T_a = T_b$, $u = 1$, $v = 0$, $\phi = \theta = 0°$, $k_1 = k_0$.

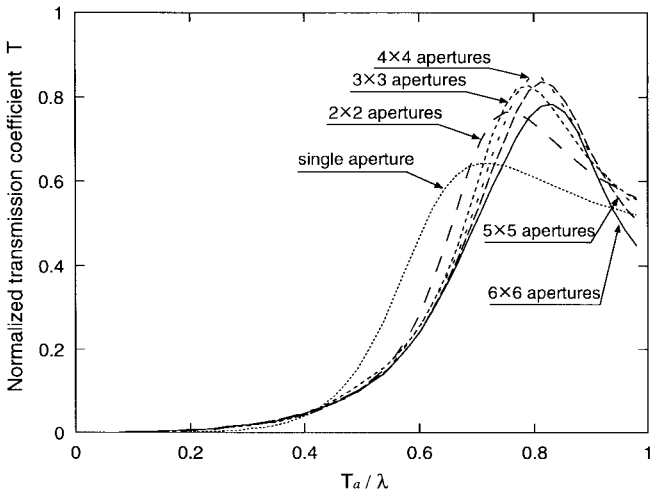

Fig. 7. Normalized transmission coefficient (averaged) versus the normalized frequency at normal incidence: $2a = 0.7 \times T_a$, $d = 0.2 \times T_a$, $b = a$, $T_a = T_b$, $u = 1$, $v = 0$, $\phi = \theta = 0°$, $k_1 = k_0$.

In Fig. 4, we illustrate the behavior of transmission coefficient τ versus incident angle for an infinitely thick rectangular aperture ($d \to \infty$, i.e., flanged rectangular waveguide antenna). Two different cases are considered when a uniform plane wave is obliquely incident on the rectangular aperture. We compare τ (equivalent to the receiving power pattern) with the radiation power pattern of the flanged rectangular waveguide antenna when the TE_{10} mode radiates from the antenna. Note that we used [12, eq. (11)–(39)] to evaluate the radiation power pattern for $2a/\lambda = 3.0$ and $2b/\lambda = 2.0$. The angular trends between τ and the radiation power pattern given in [12] are quite similar except for near grazing $\theta > 60°$. The similarity between the receiving and radiation power patterns stems from the fact that only a single mode TE_{10} is allowed to propagate in the waveguide.

In Fig. 5, we plot the behavior of τ versus the incident azimuth angle ϕ when a uniform plane wave is normally incident on an infinitely thick rectangular aperture with $a = 1.143$ cm and $b = 0.508$ cm. When $\phi = 0$, the incident E-field vector is in parallel with the y direction and maximum τ occurs. Note that three curves corresponding to $f = 7$, 10, 14 GHz show a monotonic decrease of τ to zero as ϕ increases to 90°. This is because only two modes TE_{10} and TE_{20} are allowed to propagate in the rectangular waveguide, thereby making $\tau \approx 0$ near $\phi = 90^o$. When $f = 14.8$ GHz, the TE_{01} and TE_{11} modes, in addition to the TE_{10} and TE_{20} modes, propagate inside the waveguide. Note that the presence of the TE_{01} and TE_{11} modes results in $\tau \approx 0.6$ at $\phi = 90°$.

In Fig. 6, we show the behavior of normalized transmission coefficient [$T = \tau \times (4ab/(T_a \times T_b))$] for 6 × 6 apertures versus the normalized frequency (T_a/λ). We note that T for the aperture on the corner (first aperture—$l = 0$, $k = 0$), T for the aperture near the center (15th aperture—$l = 2$, $k = 2$) and T for 36 apertures (averaged over $l = 0, \cdots, 5$ and $k = 0, \cdots, 5$) are shown. Note that T for the aperture near the center is almost the same as that for the infinite number of the apertures [14] when $T_a/\lambda < 0.8$.

In Fig. 7, we show the averaged T versus the number of apertures. As the number of apertures increases, the resonant peak shifts toward $T_a/\lambda \approx 0.84$, which is approximately that for the infinite number of apertures.

V. Conclusion

Electromagnetic wave scattering from multiple rectangular apertures in a thick conducting plane is investigated. By using the Fourier transform and the mode-matching technique, we obtain a solution in a fast-converging series form. In high-frequency limit ($\lambda \gg$ aperture dimension) the solution for a single aperture simplifies to an analytic closed form, thereby significantly reducing the computational amount. Numerical computations are performed to show the transmission and scattering behaviors of the multiple rectangular apertures. Our series solution well agrees with other existing solution for the rectangular aperture or cavity in a thick conducting plane.

References

[1] A. El-Hajj and K. Kabalan, "Characteristic modes of a rectangular aperture in a perfectly conducting plane," *IEEE Trans. Antennas Propagat.*, vol. 42, pp. 1447–1450, Oct. 1994.

[2] K. Barkeshli and J. L. Volakis, "Electromagnetic scattering from an aperture formed by a rectangular cavity recessed in a ground plane," *J. Elect. Waves Appl.*, vol. 5, no. 7, pp. 715–735, 1991.

[3] J. M. Jin and J. L. Volakis, "Electromagnetic scattering by the transmission through a three-dimensional slot in a thick conducting plane," *IEEE Trans. Antennas Propagat.*, vol. 39, pp. 1544–1550, Apr. 1991.

[4] C. C. Chen, "Transmission of microwave through perforated flat plates of finite thickness," *IEEE Trans. Microwave Theory Tech.*, vol. MTT-21, pp. 1–6, Jan. 1973.

[5] T. K. Sarkar, M. F. Costa, C. L. I, and R. F. Harrington, "Electromagnetic transmission through mesh covered apertures and arrays of apertures in a conducting screen," *IEEE Trans. Antennas Propagat.*, vol. AP-32, pp. 908–913, Sept. 1984.

[6] T. Andersson, "Moment-method calculations on apertures using basis singular functions," *IEEE Trans. Antennas Propagat.*, vol. 41, pp. 1709–1716, Dec. 1993.

[7] K. Yoshitomi and H. R. Sharobim, "Radiation from a rectangular waveguide with a lossy flange," *IEEE Trans. Antennas Propagat.*, vol. 42, pp. 1398–1404, Oct. 1994.

[8] H. H. Park and H. J. Eom, "Electrostatic potential distribution through a rectangular aperture in a thick conducting plane," *IEEE Trans. Microwave Theory Tech.*, vol. 44, pp. 1745–1747, Oct. 1996.

[9] Y. S. Kim and H. J. Eom, "Fourier-transform analysis of electrostatic potential distribution through a thick slit," *IEEE Trans. Electromagn. Compat.*, vol. 38, pp. 77–79, Feb. 1996 (correction, *ibid.*, p. 66, Feb. 1997).

[10] R. F. Harrington, *Time-Harmonic Electromagnetic Fields.* New York: McGraw-Hill, 1961, p. 130.

[11] H. H. Park and H. J. Eom, "Acoustic scattering from a rectangular aperture in a thick hard screen," *J. Acoust. Soc. Amer.*, vol. 101, no. 1, pp. 595–598, Jan. 1997.

[12] C. A. Balanis, *Antenna Theory: Analysis and Design.* New York: Harper Row, 1982, pp. 457–478.

[13] H. Baudrand, J. W. Tao, and J. Atechian, "Study of radiating properties of open-ended rectangular waveguides," *IEEE Trans. Antennas Propagat.*, vol. 36, pp. 1071–1077, Aug. 1988.

[14] S. W. Lee, G. Zarrillo, and C. L. Law, "Simple formulas for transmission through periodic metal grids or plates," *IEEE Trans. Antennas Propagat.*, vol. AP-30, pp. 904–909, Sept. 1982.

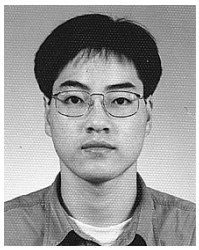

Hyun Ho Park was born in Pusan, Korea, in 1971. He received the B.S. degree in electronic engineering from Pusan National University, Pusan, Korea, in 1994, and the M.S. degree in electrical engineering from the Korea Advanced Institute of Science and Technology (KAIST), Taejon, Korea, in 1996. He is currently working toward the Ph.D. degree in electrical engineering at KAIST.

His research interests include computational electromagnetics and EMI/EMC-related problems.

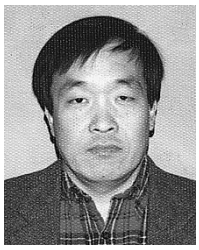

Hyo Joon Eom (S'78–M'82) received the B.S. degree in electronic engineering from Seoul National University, Seoul, Korea, in 1973, and the M.S. and Ph.D. degrees in electrical engineering from the University of Kansas, Lawrence, KS, in 1977 and 1982, respectively.

From 1981 to 1984, he was a Research Associate at the Remote Sensing Laboratory, University of Kansas. From 1984 to 1989, he was with the faculty of the Department of Electrical Engineering and Computer Science, University of Illinois, Chicago, IL. In 1989, he joined the Department of Electrical Engineering, Korea Advanced Institute of Science and Technology, where he is currently a Professor. His research interests are wave scattering and antenna.